First neutron spectrometry measurement at the HL-2A Tokamak *

YUAN Xi(袁熙)[1] ZHANG Xing(张兴)[1] XIE Xu-Fei(谢旭飞)[1] CHEN Zhong-Jing(陈忠靖)[1]
PENG Xing-Yu(彭星宇)[1] FAN Tie-Shuan(樊铁栓)[1;1)] CHEN Jin-Xiang(陈金象)[1] LI Xiang-Qing(李湘庆)[1]
YUAN Guo-Liang(袁国梁)[2] YANG Qing-Wei(杨青巍)[2] YANG Jin-Wei(杨进蔚)[2]

[1] State Key Laboratory of Nuclear Physics and Technology, Peking University, Beijing 100871, China
[2] Southwestern Institute of Physics, Chengdu 610041, China

Abstract: A compact neutron spectrometer based on the liquid scintillator is presented for neutron energy spectrum measurements at the HL-2A Tokamak. The spectrometer was well characterized and a fast digital pulse shape discrimination software was developed using the charge comparison method. A digitizer data acquisition system with a maximum frequency of 1 MHz can work under an environment with a high count rate at HL-2A Tokamak. Specific radiation and magnetic shielding for the spectrometer were designed for the neutron spectrum measurement at the HL-2A Tokamak. For pulse height spectrum analysis, dedicated numerical simulation utilizing NUBEAM combined with GENESIS was performed to obtain the neutron energy spectrum. Subsequently, the transportation process from the plasma to the detector was evaluated with Monte Carlo calculations. The distorted neutron energy spectrum was folded with the response matrix of the liquid scintillation spectrometer, and good consistency was found between the simulated and measured pulse height spectra. This neutron spectrometer based on a digital acquisition system could be well adopted for the investigation of the auxiliary heating behavior and the fast-ion related phenomenon on different tokamak devices.

Key words: compact neutron spectrometer, digital signal processing, beam-thermal neutron

PACS: 29.30.Hs, 52.70.Nc **DOI:** 10.1088/1674-1137/37/12/126001

1 Introduction

Neutron diagnostics have received growing interest in the last few decades because of its capacity to assess certain plasma parameters, such as fusion power, ion temperature, fast ion energy and spatial distributions of these parameters in the plasma core [1, 2]. The Magneto-Hydro-Dynamic (MHD) induced fast-ion losses phenomenon has been both experimentally observed and theoretically predicted [3, 4] in different Tokamak devices. Similar MHD activities, such as sawbone, ion-fishbone and long-lived bone have been observed at HL-2A Tokamak [5, 6]. It is important to measure the fast ion distribution for revealing the fast-ion related phenomena. Neutron yield and neutron energy spectrum are well correlated with the fast-ion distribution, which is widely used in the assessment of the fast-ion behavior [7–9]. At HL-2A Tokamak, neutral beam injection (NBI) heating is an important source of fast ions. At relatively low ion temperature, beam-thermal neutrons are dominant among all the neutron species. Therefore, it is of advantage to evaluate fast ions with neutron measurements. The liquid scintillator spectrometer is generally employed because of its high efficiency, good neutron/γ-ray discrimination ability and compact size with which the liquid scintillator could be located near to the device. Today, neutron spectrometers based on the liquid scintillator have been installed on Tokamak devices, such as JET [10, 11], AUG [12], FTU [13], JT-60U [14], MAST [15] and EAST [16].

In this work, a compact neutron spectrometer (CNS) based on the liquid scintillator EJ301 was developed and operated for neutron spectrum measurements at the HL-2A Tokamak. The spectrometer was well characterized and a fast digital pulse shape discrimination software was developed using the charge comparison method. For the analysis of the pulse height spectrum, dedicated numerical simulation utilizing NUBEAM [17] combined with GENESIS [18, 19] was performed to obtain the neutron energy spectrum, following which the transportation process from the plasma to the detector was evaluated with the Monte Carlo calculation code MCNP [20]. Good con-

Received 11 April 2013
* Supported by State Key Development Program for Basic Research of China (2013GB106004, 2012GB101003, 2008CB717803), National Natural Science Foundation of China (91226102) and National Science and Technology Support Program (2011BAI02B01)
1) E-mail: tsfan@pku.edu.cn

sistency was found between the simulated and measured pulse height spectra.

This paper is organized as follows. The experimental setup, calibration results of CNS and digital pulsed shape discrimination techniques are presented in Section 2. The experimental measurements and Monte Carlo analysis of CNS at HL-2A Tokamak are given in Section 3. The measured results of CNS are described in Section 4. The conclusions are presented in Section 5.

2 Energy calibration and digital pulsed shape discrimination of the liquid scintillator neutron spectrometer

The experimental arrangement of the compact neutron spectrometer is schematically shown in Fig. 1. The core cell of the CNS was a cylindrical liquid scintillator EJ301. The liquid scintillator had an active volume of near 100 cm^3(2 inch in diameter and 2 inch in length), and the thickness of the liquid scintillator was two times larger than the mean free path of 2.45 MeV protons in the sensitive material. The scintillator was optically coupled to a 2 inch Hamamatsu R329-02 photomultiplier tube (PMT) directly, and the PMT was coupled to an ORTEC 265A voltage divider. Magnetic shielding was composed of an additional 0.8 mm μ-metal shield. The anode signals of CNS were sent into a high-speed digitizer of model Agilent U1065A through a 2 m long coaxial-cable. Agilent U1065A was a quad-channel 10-bit digitizer with a sampling rate of up to 8 Gsamples/s and a full scale range of 50 mV to 5 V. Raw data were transferred to a PC over an ethernet connection using UDP/IP.

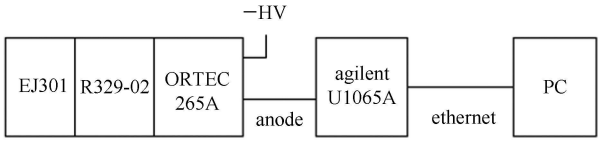

Fig. 1. Schematic diagram of the compact neutron spectrometer.

The pulse height spectrum (PHS) of CNS could reflect the light output for secondary particles such as electrons and protons. In addition it could be considered as the photon and neutron spectra folded with the response matrix. It is important to get the response matrix specifically for this spectrometer. Therefore, calibration experiments were established with γ-ray and neutron sources.

Energy calibration was performed with γ-ray sources (^{137}Cs, ^{54}Mn and ^{22}Na) to establish the relationship between pulse heights Q_α and electron equivalent energy E_{ee}, expressed by

$$Q_\alpha = G(E_{ee} - E_0), \tag{1}$$

where Q_α is the charge integral of the pulse in a 130 ns time range, G is the calibration factor and E_0 is the nonlinearity from the quenching effects and other factors. G and E_0 were obtained by iterative fitting between experimental and theoretical γ-ray spectra calculated by the Monte Carlo code GRESP [21], which was developed by the Physikalisch-Technische Bundesanstalt (PTB). Three experimental configurations of the detector and digitizer (high voltages and full ranges) were used to cover the neutron energy ranging from 1 MeV to 17 MeV, and the energy calibration was completed for each configuration.

The relationship between the light output function of recoil protons and the electron equivalent energy is strongly nonlinear [22], and this relationship is different for each spectrometer. Fifteen quasi-monoenergetic neutron fields were generated by nuclear reactions via the 4.5 MV Van de Graaff accelerator at Peking University, including Li^7(p, n)Be^7 (1.14 and 1.38 MeV), T(p, n)^{3}He (1.60, 1.90, 2.14 and 2.40 MeV), D(d, n)^{3}He (2.95, 3.95, 4.11, 5.21 and 6.0 MeV) and T(d, n)^{4}He (14.1, 15.1, 16.1 and 17.7 MeV). The quasi-monoenergetic neutrons with specific energies were selected by the time-of-flight method, which could reduce the ratio of scattered neutrons remarkably. The injected neutron energy and broadenings were calculated by the code TARGET [23], which was also developed by the PTB. They were adopted as the input parameters of the Monte Carlo code NRESP7 [24]. Iterative calculations and fittings were established to obtain the nonlinear light output function and pulse height resolution dL/L. The latter can be expressed as

$$\mathrm{d}L/L = \sqrt{7.5^2 + 8.08^2/L + 0.2^2/L^2}. \tag{2}$$

The comparison between the experimental and calculated pulse height spectra of ^{54}Mn and three quasi-monoenergetic neutron fields are shown in Fig. 2.

The radiation field around the tokamak device is a mixed neutron/γ-ray field. Sometimes the photon flux is even higher than the neutron flux. These photons are produced by the interactions of runaway electrons with the plasma chamber wall and inelastic scattering and capture reactions of neutrons with the tokamak device. Therefore, a good discrimination technology should also be developed for the liquid scintillator because of its sensitivity to photons. The total maximum count rate of the detector must be high enough to leave free space for the neutron counting. A new digital acquisition and discrimination system was developed for these two objectives.

The difference in the shapes of the light pulses generated by neutrons and photons in EJ301 liquid scintillator could be used for the discrimination between neutron and photon events. The light pulses in the scintillator are

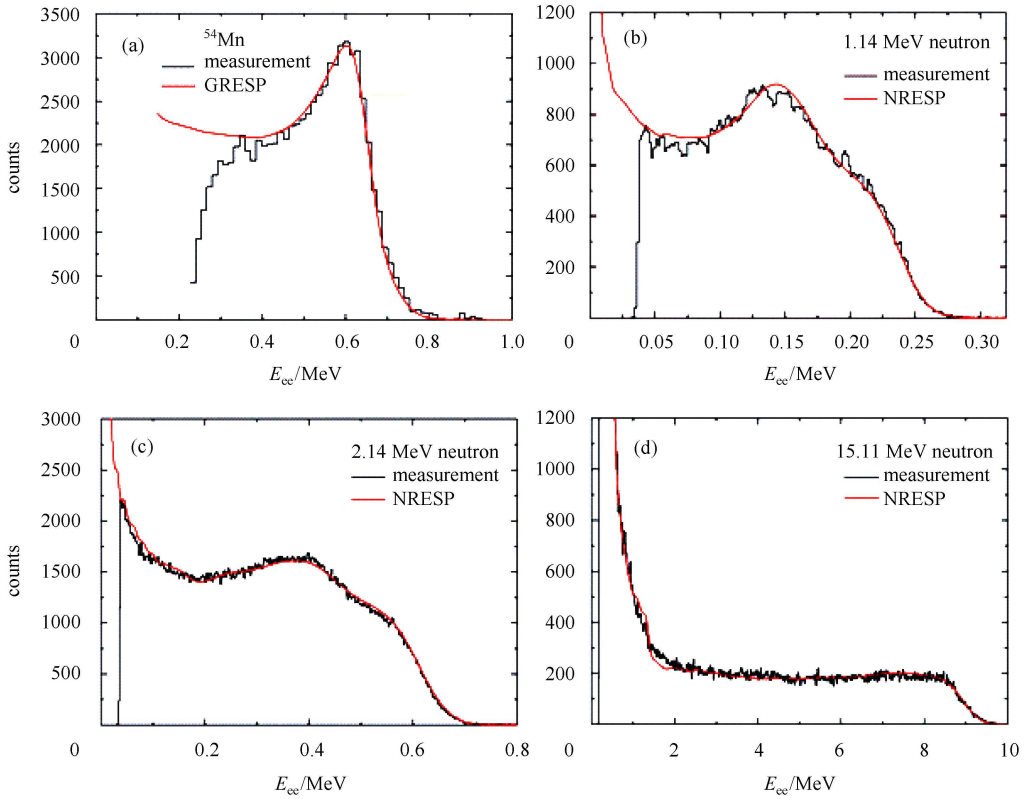

Fig. 2. (color online) Comparisons of calculated (red line) and measured (black histograms) spectra. The measured and calculated results from the code GRESP for ^{54}Mn γ-ray source (a), and the measured and calculated results from the code NRESP for 1.14 MeV (b), 2.14 MeV (c), 15.11 MeV (d) quasi-monoenergetic neutron sources, respectively.

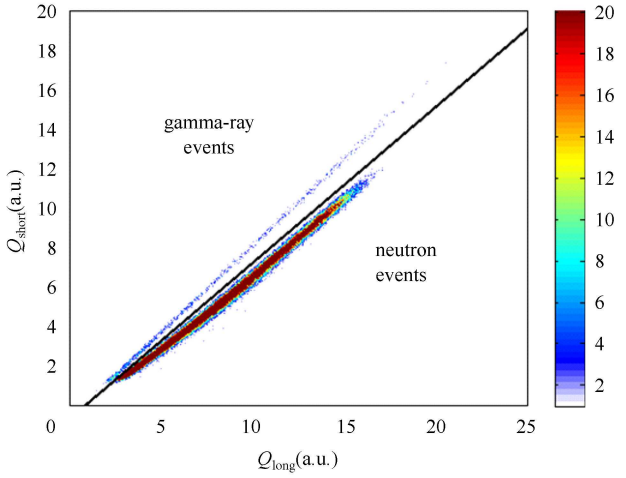

Fig. 3. (color online) Plot of $Q_{\rm long}$ versus $Q_{\rm short}$ for 2.40 MeV neutron sources. The straight line used to separate neutron events from photon events is shown in the figure.

combinations of similar fast scintillation components (approximately 4 ns to 5 ns) and different slow scintillation components (approximately 100 ns to 200 ns). The DPSD method used in this work was a typical charge comparison method [25]. Each pulse was integrated for two time lengths as charge values $Q_{\rm long}$ and $Q_{\rm short}$, which denote the total and fast components, respectively. With the same $Q_{\rm short}$ value, the corresponding $Q_{\rm long}$ value for neutrons is larger than that for γ-rays. For this EJ301 CNS, the time lengths of short and long time windows were optimized to be 15 ns and 130 ns, respectively. The DPSD result of 2.40 MeV quasi-monoenergetic neutron sources from the T(p, n)^{3}He reaction is shown in Fig. 3. Other DPSD methods based on both time and frequency domain analysis have also been developed [26, 27].

3 Experimental measurements and Monte Carlo analysis at HL-2A Tokamak

The main plasma discharge parameters of the HL-2A Tokamak are nominally as follows: major radius R=1.65 m, minor radius a=0.4 m, $I_{\rm P}$=400 kA, $B_{\rm T}$=2.65 T, and $n_{\rm e0}\sim6.0\times10^{19}$ m^{-3}. During plasma discharges, neutrons are generally produced by the reaction between fusion deuteron fuel ions. Most of the neutrons are from the beam-thermal component under NBI that can generate numerous fast fuel ions. Therefore, the neu-

tron energy distribution could be related to the fast ion energy distribution. Moreover it is possible to assess the behavior of fast ions via neutron measurements.

For the application of CNS at HL-2A Tokamak, specific shielding was developed for radiation and magnetic shielding. The CNS spectrometer was shielded from scattered neutrons by a 40 cm pure polyethylene in the front region. To reduce the weight and size of shielding, the thickness of polyethylene at the back and side regions were 15 cm, where the fluence of scattered neutrons was lower. However, polyethylene can produce 2.226 MeV γ-rays from the neutron capture reaction, for which a close lead shield of more than 20 cm thickness was located between the polyethylene and the CNS. A 1.3 cm DT4C soft iron cylinder between the lead shield and a 2 mm permalloy around the spectrometer were employed to shield the detector from the HL-2A magnetic fields, which was less than 0.02 T at the CNS location. The measured spectra of the ^{137}Cs time by time showed that the gain of the detector was stable during discharges. Considering the spatial layout, the shielding was finally located at the mid-plane of HL-2A Tokamak, and behind the soft X-ray system in the radial direction. The distance between the detector and the nearest plasma core was 3 m, and the sight line of the spectrometer could cover the entire small radius. A photo of shielding in the experimental hall is shown in Fig. 4.

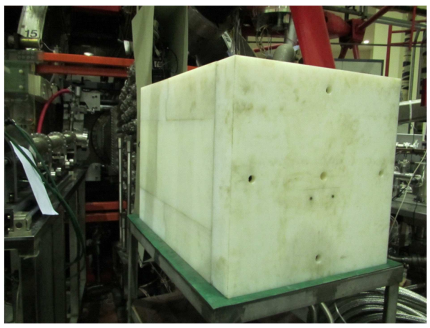

Fig. 4. Scene photo of CNS shielding around the HL-2A Tokamak.

Figure 4 shows the complex environment around the CNS. This environment would give rise to the neutron spectrum variations from the plasma to the detector, especially for the components in the line of sight. A 3-D MCNP model was built to simulate the softening process of the energy spectrum. This model included the main parts of the tokamak, the experimental hall, the faced window, the soft X-ray system and the whole neutron spectrometer. The 2-D schematic diagrams of MCNP model are shown in Fig. 5.

The emission neutron spectrum was calculated by the Code NUBEAM and the Monte Carlo code GENESIS. NUBEAM simulations were performed for the magnetic

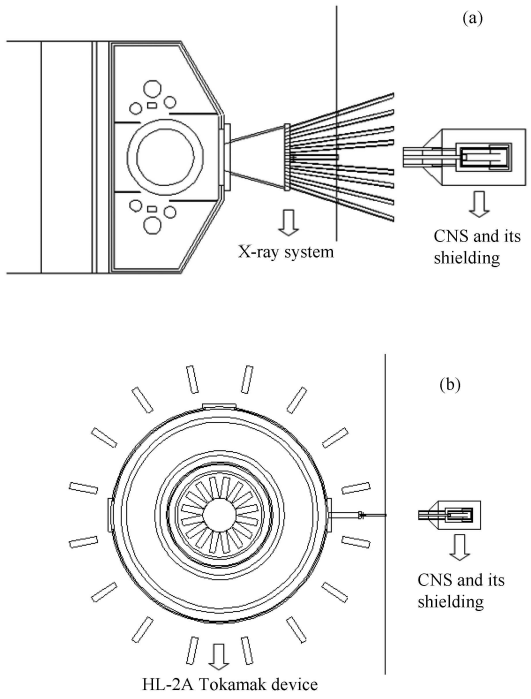

Fig. 5. Schematic model of the experimental setup of the neutron spectrometer at the HL-2A Tokamak with the elevation view (a) and the plane view (b).

equilibrium of the HL-2A shot 20016. The temperature and density profiles, as functions of the normalized toroidal flux surface coordinate, are assumed to be given by

$$T(\rho) = [T(0)-T(1)](1-\rho^2)+T(1), \quad (3)$$

$$n(\rho) = [n(0)-n(1)](1-\rho^2)^{0.5}+n(1), \quad (4)$$

where $T_{\rm e}(0)$, $T_{\rm i}(0)$ and $n(0)$ are the temperature and density in the plasma core, and they were set to 1 keV, 0.8 keV and 2×10^{19} m^{-3}, respectively, $n(1)$=$0.1\times n(0)$ and $T(1)$=$0.1\times T(0)$ were further assumed. The plasma dilution was represented by an effective charge number $Z_{\rm eff}$=2.5. Both neutral beam lines had injection energy of 40 keV and the total power was assumed to be operated at a steady state of 1 MW. The output of the NUBEAM calculation consisted of energy distributions of the beam ions $F_{\rm NBI}$ which were used as the input for calculations of the D-D neutron spectrum with the code GENESIS. The code GENESIS, which is based on classical kinematics, is able to calculate the energy spectrum of neutron and γ-rays emitted from several nuclear reactions in the plasma, starting from the reactant energy distributions, reaction cross sections and plasma profiles. Both neutron spectrum generated in the plasma and the neutron spectrum after transmission are compared in Fig. 6. In order to increase the calculation efficiency, the cut energy for neutrons in the code MCNP was set up to 0.8 keV,

which was coordinated with the lower threshold of measurements.

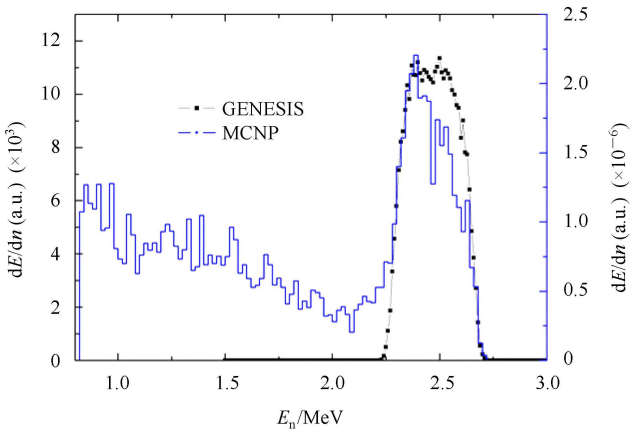

Fig. 6. (color online) Comparison of the input neutron spectrum from the code GENESIS (black point) and the output neutron spectrum from the MCNP code (blue line).

4 Experimental results

In some large Tokamak devices such as JET and ITER, neutron spectrometers have to acquire and process mass data in a short time (mostly less than 10 s). At HL-2A Tokamak, the neutron yield is less than 10^8/s without NBI auxiliary heating and the neutron yield will explosively increase by more than 10^4 times with NBI heating. The maximum count rate for analog electronic modules is usually less than 100 kHz, which could not meet the need of fusion neutron measurements. The Agilent U1065A digitizer has two working modes: the trigger mode and the continuous mode. For the trigger mode, the dead time for each pulse is 1.8 μs, indicating that the maximum count rate is below 500 kHz with the 200 ns record length, which is not high enough for fusion neutron measurements. For DPSD, the time resolution is set to 1 ns or 2 ns because of the 4 ns to 5 ns rise time of liquid scintillator signals. Therefore, for the largest 2 GB RAM, the record time is 1 s to 2 s. The time interval of NBI is about 500 ms, and without NBI the neutron flux decreases dramatically. In this case, flash ADC was set to 1 Gsamples/s sampling and it began to acquire data 100 ms after the external trigger signal which is the clock of HL-2A data acquiring system. The advantage of continuous mode was that the digitizer was no longer the limit of maximum count rate and the data transmission speed no longer needs to be considered. Instead, more work must be focused on the DPSD for the pile-up signals and the strike of PMT for a large current. When the CNS was located outside the shielding, the PMT tube did not work after near 50 ms of NBI heating. The DPSD result of discharge #20016 is shown in Fig. 7. Note that the γ-ray energy is much higher than the neutron energy, which can even reach 8 MeV.

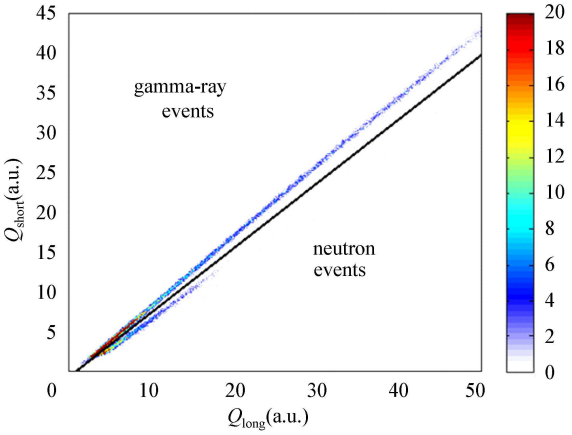

Fig. 7. (color online) Plot of $Q_{\rm long}$ versus $Q_{\rm short}$ for HL-2A discharge #20016. The straight line used to divide neutron events from photons events is indicated in the figure.

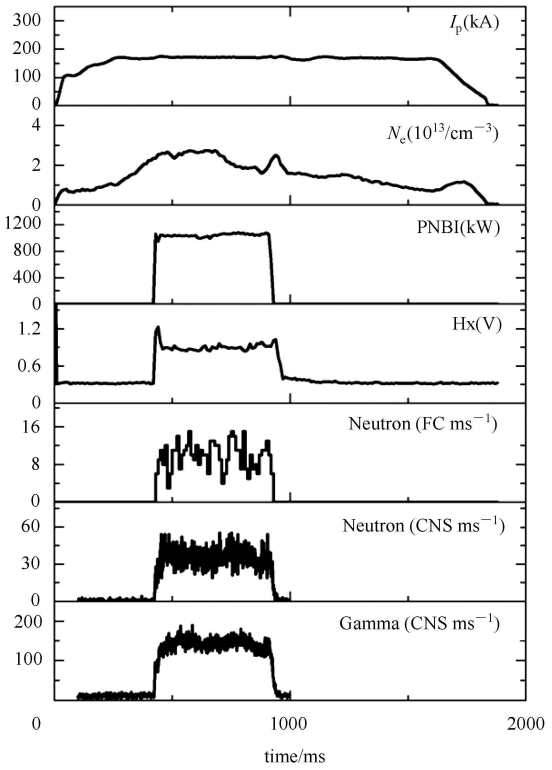

Fig. 8. Time traces of plasma current, electron density, NBI power, hard X-ray, neutron and γ-ray count rate during HL-2A plasma discharge #20016.

The time traces of plasma current $I_{\rm p}$, electron density $n_{\rm e}$, NBI power, hard X-ray, neutron fluence monitored by a ^{235}U fission chamber and the neutron, and γ-ray fluence from the CNS are demonstrated in Fig. 8. Note that the γ-ray flux with higher energy is at least three times

more than the neutron flux, and the maximum ratio is 10 in the experiment scenarios. The time trace of the neutron fluence monitored by the CNS is similar to the one monitored by the fission chamber, and both of them are directly related to the NBI power. The total count rate of the CNS is near 200 kHz.

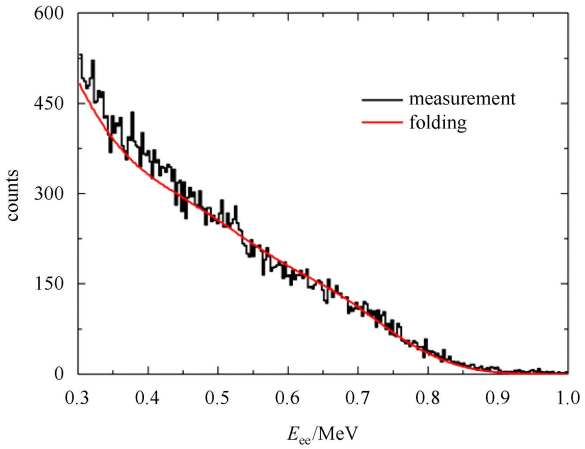

Fig. 9. (color online) Comparison of measured pulse height spectra (black histogram) of nine discharges (#20016-20025 except #20021) and calculated folding pulse height spectra (red line).

In order to increase the statistics of the measured spectra, pulse height spectra of nine similar discharges (#20016-20025 except #20021) were combined. The neutron spectrum detected at the CNS was the same as the result shown in Fig. 6. The theoretical pulse height spectrum was obtained by folding the neutron energy spectrum with the detector response matrix, and it was generally consistent with the experimental result, as illustrated in Fig. 9. This finding indicates that neutron emission is dominated by the beam-plasma reactions.

5 Conclusions

A compact neutron spectrometer was developed and built at HL-2A Tokamak for neutron emission spectrum measurements. This spectrometer worked well in the complex environment and high photon and neutron scattering background. The maximum count rate of the spectrometer was up to 1 MHz. For the NBI heating at HL-2A Tokamak, the beam-thermal neutron component was calculated by the code NEUBEAM and GENESIS, and detailed modeling of neutron transmission from the plasma core to the detector was performed using the MCNP code. The experimental pulse height spectrum fitted well with the theoretical one. Future work will focus on the analysis of neutron spectra in different heating scenarios.

The authors are very grateful to the HL-2A operation Team for their help during the experiment on HL-2A. The authors are also grateful to Prof. R. Nolte and Dr. M. Reginatto of PTB for their help in using the GRESP, NRESP and TARGET codes. The authors are grateful to Prof. Jianyong Wang of Peking University for the accelerator operation.

References

1 Wolle B. Physics Reports, 1999, **312**: 1
2 Jarvis O N. Plasma Phys. Control. Fusion, 1994, **36**: 209
3 Hellesen C, Gatu Johnson M, Sundén E A et al. Nucl. Fusion, 2010, **50**: 084006
4 White R B, Chance M S. Phys. Fluids, 1984, **27**(10): 2455
5 CHEN W, DING X T, LIU Yi et al. Nucl. Fusion, 2010, **50**: 084008
6 YANG Q W, LIU Yong, DING X T et al. Nucl. Fusion, 2007, **47**: 635
7 Källne J, Ballabio L, Gorini G et al. Phys. Rev. Lett., 2001, **85**: 1246
8 Hellesen C, Gatu Johnson M, Sundén E A et al. Nucl. Fusion, 2010, **50**: 022001
9 Hellesen C, Albergante M, Sundén E A et al. Nucl. Fusion, 2010, **52**: 085013
10 Zimbal A, Reginatto M, Schuhmacher H et al. Rev. Sci. Instrum., 2004, **75**: 3553
11 Esposito B, Bertalot L, Marocco D et al. Rev. Sci. Instrum., 2004, **75**: 3550
12 Giacomelli L, Zimbal A, Tittelmeier K et al. Rev. Sci. Instrum., 2011, **82**: 123504
13 Esposito B, Kaschuck Y, Rizzo A et al. Nucl. Instrum. Methods Phys. Res. A, 2004, **518**: 626
14 Shibata Y, Hoek M, Nishitani T et al. Japan Atomic Energy Research Institute Report, JAERI-Conf., 2000–004.130–133
15 Cecconello M,Turnyanskiy M, Conroy S et al. Rev. Sci. Instrum., 2010, **81**: 10D315
16 LI X L, WAN B N, ZHONG G Q et al. Plasma Phys. Control. Fusion, 2010, **52**: 105006
17 Pankin A, McCune D, Bateman G et al. Computer Physics Communications, 2004, **159**: 157
18 Ballabio L. Calculation and Measurement of the Neutron Emission Spectrum Due to Thermonuclear and Higher-Order Reactions in Tokamak Plasmas (Ph. D. Thesis). Uppsala: Faculty of Sciences and Technology, Uppsala University, 2003
19 Tardocchi M, Nocente M, Proverbio I et al. Phys. Rev. Letters, 2012, **107**: 205002
20 X-5 Monte Carlo Team. MCNP-A General Monte Carlo N-particle Transport Code, Version 5, Report LA-UR-03-1987. Los Alamos National Laboratory, New Mexico, United States of America, 2003
21 Dietze G, Klein H. Nucl. Instrum. Methods, 1982, **193**: 549
22 KleinHorst, NeumannSonja. Nucl. Instrum. Methods Phys. A, 2002, **476**: 132
23 Schlegel D. PTB Laboratory Report, PTB-6.42-05-2. Braunschweig, Germany, 2005
24 Dietze G, Klein H. PTB LaboratoryReport, PTB-ND-22, Braunschweig, Germany, 1982
25 Wolski D, Moszyiiski M, Ludziejewski T et al. Nucl. Instrum. Methods Phys. A, 1995, **360**: 584
26 ZHANG Xing, YUAN Xi, XIE Xu-Fei et al. Nucl. Instrum. Methods Phys. A, 2012, **687**: 7
27 XIE Xu-Fei, ZHANG Xing, YUAN Xi et al. Rev. Sci. Instrum., 2012, **83**: 093507